Vesicular Stomatitis Virus Glycoprotein Displaying Retrovirus-Like Particles Induce a Type I IFN Receptor-Dependent Switch to Neutralizing IgG Antibodies[1]

Patricia Bach,* Elisabeth Kamphuis,[2]* Bernhard Odermatt,† Gerd Sutter,‡ Christian J. Buchholz,§ and Ulrich Kalinke[3]*

Vesicular stomatitis virus (VSV) infection rapidly induces IFN-$\alpha\beta$ that confers initial survival, whereas long-term protection is mediated by neutralizing IgG responses. Because coadministration of IFN-$\alpha\beta$ can enhance Ab responses against soluble Ags, we addressed whether virus-induced IFN-$\alpha\beta$ also had an impact on the induction of neutralizing Ab responses. To this end, we generated apathogenic retrovirus-like particles (VLP) displaying the VSV gp (VLP-VSV). Reminiscent of live VSV, VLP-VSV induced VSV-neutralizing IgM responses that switched to IgG in a T help-dependent manner. In type I IFN receptor-deficient (IFNAR$^{-/-}$) mice, VLP-VSV injection elicited neutralizing IgM, whereas the IgG switch was absent. The lack of subclass switch was associated with a reduced germinal center reaction. Conditional knockout mice with a lymphocyte-specific IFNAR ablation showed normal Ab responses against VLP-VSV, as well as against live VSV. Thus, IFNAR triggering critically promoted the T help-dependent subclass switch of virus-neutralizing Ab responses against VLP-VSV. Interestingly, in the context of VLP-VSV as well as VSV immunization, IFNAR triggering of B lymphocytes did not play a critical role. *The Journal of Immunology,* **2007, 178: 5839–5847.**

Within the first hours after virus infection, a number of pathogen-associated molecular patterns that trigger innate immunity and cytokines, such as type I IFN, are produced that ensure initial survival of the host (1). Vesicular stomatitis virus (VSV)[4] infection induces maximal IFN-$\alpha\beta$ levels after ~12 h. At later time points, IFN-$\alpha\beta$ levels decline and reach background levels by day 2 (2, 3). Rapid IFN-$\alpha\beta$ induction is critically required for the initial survival, as demonstrated by VSV-infected IFN receptor-deficient (IFNAR$^{-/-}$) mice that succumb to low-dose infection within few days, whereas wild-type (WT) mice usually survive infections with >6 magnitudes higher virus doses (4). Furthermore, protection requires the induction of VSV-neutralizing Ab responses, as indicated by B cell-deficient mice that succumb to VSV infection between days 5 and 7 (5). Finally, long-term protection is further supported by the subclass switch of neutralizing IgM to IgG. This was demonstrated by mice depleted of CD4$^+$ T cells that mounted VSV-neutralizing IgM responses, but did not show an IgG subclass switch and showed an increased sensitivity to lethal VSV infection (6).

Several lines of evidence pointed toward an impact of IFN-$\alpha\beta$ on Ab responses. In in vitro studies, B cells treated with suboptimal anti-IgM showed an enhanced IgM production upon costimulation with IFN-$\alpha\beta$ (7). More strikingly, in vivo experiments established an adjuvant effect of IFN-$\alpha\beta$ leading to improved Ab responses. In this context, it was shown that IgG responses toward an influenza subunit vaccine (8) and against the soluble protein chicken γ-globulin (CGG) (9, 10) were enhanced by type I IFN stimulation. In the latter model, Le Bon et al. (9–11) demonstrated that injection with CGG devoid of adjuvans induced only very weak Ab responses, whereas coinjection of CGG and IFN-$\alpha\beta$ induced significant CGG-specific IgM and IgG responses. Under these experimental conditions, IFN-$\alpha\beta$ stimulation of dendritic cells (DCs), as well as of B and T cells, played a critical role.

Depending on the virus infection analyzed, virus-induced type I IFN may or may not have an impact on anti-viral Ab responses. Van den Broek et al. (13) demonstrated that after infection with the noncytopathic lymphocytic choriomeningitis virus (LCMV), which induces significant type I IFN responses (12), IFNAR$^{-/-}$ mice and WT controls mounted similar NP-specific Ab responses of a comparable magnitude and isotype pattern. In contrast, after infection with a low pathogenic influenza virus strain that is similarly cleared in IFNAR$^{-/-}$ and WT mice, IFNAR signaling was one of the first direct stimulatory signals required for local lymph node B cells to mount Ab responses. In this model, IFNAR$^{-/-}$ mice, which showed a reduced frequency of influenza-specific B cells, produced a changed isotype pattern of influenza-specific Abs, and the differentiation of activated B cells to Ab-secreting plasma cells was hampered (14). Recent VSV infection studies conducted in mice carrying adoptively transferred transgenic

*Division of Immunology, Paul-Ehrlich-Institut, Langen, Germany; †Department of Pathology, University Hospital Zürich, Zürich, Switzerland; ‡Division of Virology, Paul-Ehrlich-Institut, Langen, Germany; and §Division of Medical Biotechnology, Paul-Ehrlich-Institut, Langen, Germany

Received for publication September 26, 2006. Accepted for publication February 13, 2007.

The costs of publication of this article were defrayed in part by the payment of page charges. This article must therefore be hereby marked *advertisement* in accordance with 18 U.S.C. Section 1734 solely to indicate this fact.

[1] This work was supported by the German Research Council (SFB432, B15), the Volkswagen Foundation, and the European Community (PRIOVAX, Contract QLK2-CT-2002-81399).

[2] Current address: Testing Laboratory for In Vitro-Diagnostics, Paul-Ehrlich-Institut, Langen, Germany.

[3] Address correspondence and reprint requests to Dr. Ulrich Kalinke, Division of Immunology, Paul-Ehrlich-Institut, Langen, Germany. E-mail address: kalul@pei.de

[4] Abbreviations used in this paper: VSV, vesicular stomatitis virus; CGG, chicken γ-globulin; DC, dendritic cell; EGF, epidermal growth factor; FDC, follicular DC; GC, germinal center; int, intermediate; LCMV, lymphocytic choriomeningitis virus; MLV, murine leukemia virus; PNA, peanut hemagglutinin; VLP, retrovirus-like particle; VLP-EGF, EGF-displaying VLP; VLP-VSV, VLP displaying VSV gp; VSV-G, VSV gp; VSV-IND, VSV serotype Indiana; WT, wild type.

VSV-specific B cells suggested that IFNAR signaling of B cells enhanced plasma blast formation and increased IgM responses (15). However, in these studies, the adoptively transferred IFNAR-deficient B cells expressing a transgenic BCR competed with endogenous IFNAR-competent B cells. Therefore, the overall neutralizing Ab responses were rather similar, irrespective of whether IFNAR-deficient or IFNAR-competent transgenic B cells were transferred. Thus, the question of whether IFNAR signaling had an impact on the induction of virus-neutralizing B cell responses remained elusive.

To address this issue, we generated retrovirus-like particles (VLP) displaying VSV gp (VSV-G) (VLP-VSV) that are entirely replication deficient and thus are not infective. Compared with UV-inactivated VSV that primarily induces IgM responses within a broad range of doses, we showed in this study that VLP-VSV is highly immunogenic and induces VSV-neutralizing IgM responses that switch to the IgG subclass. Furthermore, we found that IFNAR triggering only marginally affected VLP-VSV-induced neutralizing IgM responses, whereas it was critically required to promote the IgG switch. The analysis of conditional knockout mice with a lymphocyte-specific IFNAR deletion revealed that IFNAR triggering of lymphocytes did not play a crucial role, neither upon VLP-VSV nor VSV immunization.

Materials and Methods

Mice

CD19-Cre$^{+/-}$CD4-Cre$^{+/-}$IFNAR$^{flox/flox}$ (IFNAR-BT), CD19-Cre$^{+/-}$IFNAR$^{flox/flox}$ (IFNAR-B), and CD4-Cre$^{+/-}$IFNAR$^{flox/flox}$ (IFNAR-T) mice have been obtained by intercrossing conditional IFNAR mice (IFNAR$^{flox/flox}$ (3, 10, 11)) and CD4-Cre and/or CD19-Cre transgenic mice expressing the recombinase Cre specifically in T cells (16) or B cells (17), respectively. All of these mice have been 10-fold backcrossed to the C57BL/6 background before they were used for matings. Type I IFN receptor-deficient (IFNAR$^{-/-}$) mice (4) have been 20-fold backcrossed to the C57BL/6 background. Mice were kept under specific pathogen-free conditions at the central mouse facility of the Paul-Ehrlich-Institut. Unmutated C57BL/6 mice, also referred to as WT, were purchased from Charles River Laboratories or were bred at the Paul-Ehrlich-Institut. For experimental mouse work, 6- to 8-wk-old animals were used. Experiments were conducted in compliance with the regulations of the German animal protection law.

Viruses and production of VLP

VSV serotype Indiana (VSV-IND; Mudd-Summers isolate) was originally obtained from D. Kolakofsky (University of Geneva, Geneva, Switzerland), and was grown on BHK cells in MEM supplemented with 5% FCS to obtain virus stocks containing 10^9 PFU/ml. UV inactivation was performed with a UV irradiator (Herolab; CL-1) at 300 mJ. For the production of VLP, human embryonic kidney-293FT cells (Invitrogen Life Technologies) cultivated in DMEM supplemented with 10% FCS were transiently cotransfected with the murine leukemia virus (MLV) *gag/pol* expression plasmid pHIT60 (18) in combination with the VSV-G or epidermal growth factor (EGF) display constructs pmDG (19) and pDEGF, respectively, using lipofectamine, according to the manufacturer's instruction (Invitrogen Life Technologies). Cell culture supernatants were harvested 48 h after transfection, and particles were concentrated by low speed centrifugation (3600 rpm, 4°C; Biofuge Heraeus). Pelleted virus was resuspended in PBS and used for electron microscopy, ELISA analysis, and immunizations. To estimate absolute particle numbers, reverse-transcriptase units were determined from VLP preparations. Assuming that 1 reverse-transcriptase unit corresponded to 3×10^9 VLPs (20), $\sim 10^9$ particles were used for typical immunization experiments. For equilibration of particle preparations, ELISA tests were performed, as described previously (21).

Electron microscopy

For immunonegative staining, 10 μl of virus suspension was adsorbed to glow discharged carbon-coated Formvar grids for 2 min. After rinsing in PBS, grids were incubated with a polyclonal anti-VSV-G rabbit antiserum at 1/1000 dilution for 15 min. After washing, grids were incubated with a 10-nm-diameter gold particle-labeled goat anti-rabbit IgG Ab (Biocell Laboratories) at 1/50 dilution for 15 min. Finally, immunolabeled samples were negatively stained with 2% uranylacetate for 10 s. Electron microscopy preparations were examined in a Zeiss EM 109 or 902 electron microscope.

Analysis of VSV-specific serum binding by ELISA

Purified VSV-IND was prediluted 1/10,000 and coated in 0.1 M $NaHCO_3$ (pH 9.6), on 96-well ELISA plates (Nunc). After blocking with 5% BSA, 20-fold prediluted serum was serially 3-fold diluted ($20 \times \log_3$) in PBS, 0.1% Tween 20, and 1% BSA, and added for 2 h at room temperature to the ELISA plates. Upon thorough washing, the HRP-conjugated polyclonal rabbit Ab directed against mouse Ig of the M or G subclasses (anti-mouse IgM, anti-mouse IgG; Zymed Laboratories) was added in a 1/1000 dilution. After 1-h incubation at room temperature, plates were washed, and for the detection of bound HRP-coupled Abs substrate was added (0.5 mg/ml 2.2′-azino-di-ethyl-benzothiazolinsulfonat (Roche) in 0.1 M NaH_2PO_4 (pH 4) and 30% H_2O_2). The OD was determined at a wavelength of $\lambda = 405$ nm.

To analyze molecules displayed by VLP, 96-well ELISA plates (Nunc) were coated with graded concentrations of purified VLP-VSV or EGF-displaying VLP (VLP-EGF) that were prediluted 1/10 in 0.1 M $NaHCO_3$ (pH 9.6) and subsequently serially 3-fold diluted ($10 \times \log_3$). For coating of VSV, purified virus was 1/1000 prediluted, serially 3-fold diluted, and then transferred to 96-well ELISA plates. After overnight incubation, unspecific binding was blocked using 5% BSA. For detection of surface Ags, the mouse VSV-G-specific mAb VI24 (22) prediluted 1/200 or MLV-specific anti-p30 antiserum diluted 1/1000 in PBS, 0.1% Tween, and 1% BSA was added for 2 h at room temperature. Upon thorough washing, bound Ab was decorated using 1/1000 diluted HRP-conjugated rabbit anti-mouse IgM + G + A Ab (Zymed Laboratories).

Depletion of CD4$^+$ T cells

Three days and 1 day before immunization with VLP-VSV or VSV, mice were injected i.p. with a dose of 500 μg of GK1.5 mAb (Harlan Bioproducts) per injection. Depletion efficiency, as determined by FACS analysis of peripheral blood, typically exceeded 99.9% and resulted in the complete inhibition of the IgM to IgG switch of VSV-neutralizing serum Abs observed in VSV-infected mice.

VSV neutralization assay

Serial 2-fold dilutions of 1/40 prediluted serum samples were mixed with equal volumes of VSV containing 10^2 PFU, and the mixtures were incubated for 90 min at 37°C in an atmosphere containing 5% CO_2. A total of 100 μl of the mixtures was transferred onto Vero cell monolayers in 96-well plates and incubated for 1 h at 37°C. Monolayers were overlaid with 100 μl of MEM containing 1% methylcellulose, and incubated for 24 h at 37°C. Then the overlay was removed, and the monolayer was fixed and stained with 0.5% crystal violet dissolved in 5% formaldehyde, 50% ethanol, and 4.25% NaCl. The serum dilution reducing the number of plaques by 50% was taken as titer (23). To determine IgG titers, undiluted serum was treated with an equal volume of 280 mM 2-ME for 1 h at room temperature before samples were processed, as described above.

Immunohistology

Freshly removed organs were embedded in Tissue Freezing Medium (Leica Microsystems) and snap frozen by submersing samples for several minutes in liquid nitrogen. Tissue sections of 5 μm thickness were cut in a cryostat, placed on siliconized glass slides, air dried, fixed with acetone for 10 min, and stored at −70°C. Immunohistological stainings were performed, as described previously (24), except for detection of germinal center (GC) cells that was done by using biotinylated peanut hemagglutinin (PNA; Vector Laboratories). For staining of follicular DCs (FDC), rehydrated tissue sections were incubated with rat mAbs clone FDC-M1 (BD Biosciences). Staining was revealed by the ABC/peroxidase method (DakoCytomation).

Detection of GC B cells by FACS analysis

Spleens were removed, and single-cell suspensions were prepared. After RBC lysis by treatment with red blood lysing solution (BD Biosciences), splenocytes were incubated with biotinylated PNA (Vector Laboratories) in FACS buffer (PBS containing: 2% FCS, 0.03% NaN_3, and 20 mM EDTA) at 4°C for 15 min. After extensive washing with FACS buffer, cells were stained with a mixture of streptavidin-PE (BD Biosciences), PECy5.5-B220 Ab (Caltag Laboratories), FITC-conjugated anti-CD21 (BD Biosciences), and allophycocyanin-conjugated anti-CD23 (Caltag Laboratories) at 4°C for 15 min in FACS buffer. After washing, samples were analyzed on a FACS BD LSR II (BD Biosciences) using BD FACS Diva software (BD Biosciences).

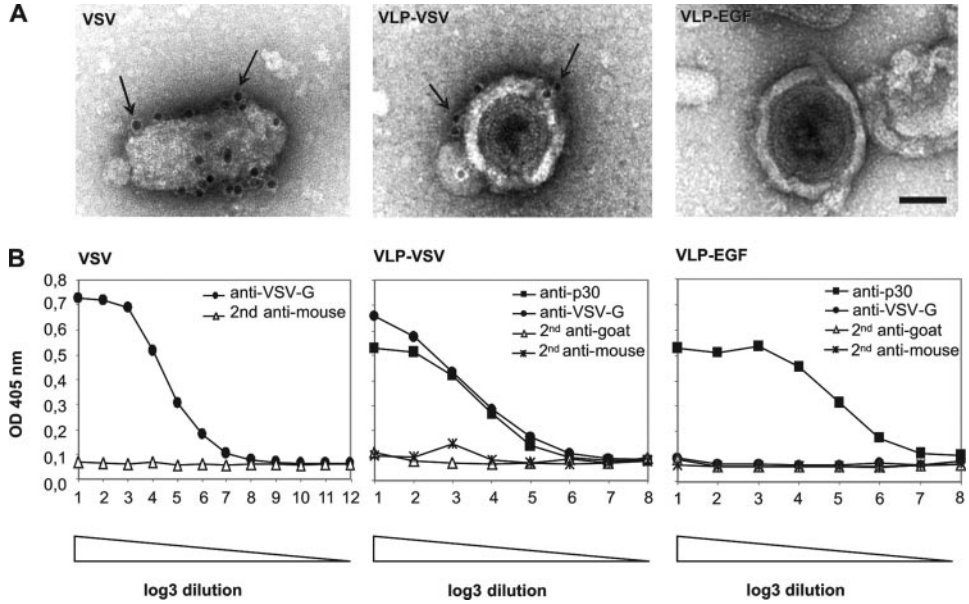

FIGURE 1. Characterization of VLP-VSV or EGF compared with VSV. *A*, Analysis of VSV-G expression by immunoelectron microscopy. Samples of VSV, VLP-VSV, and VLP-EGF were applied to glow-discharged carbon-coated Formvar grids. VSV-G was labeled by a polyclonal anti-VSV-G rabbit serum and a 10-nm-diameter gold particle-labeled anti-rabbit IgG (arrowheads). The bar is equivalent to 50 nm. *B*, Analysis of VSV-G expression by an ELISA method. ELISA plates were coated in $\log_3$ dilution steps with graded concentrations of VLP-EGF, VLP-VSV, and VSV. After blocking of unspecific binding, plates were incubated with the VSV-G-specific mouse mAb VI24 (●) or with MLV-specific goat anti-p30 polyclonal serum (■). Bound Abs were detected by an anti-mouse IgG2a-HRP Ab or anti-goat IgG-HRP.

To determine absolute counts of spleen cell subsets, a defined volume of spleen cells was mixed with an equivalent volume of counting beads (Caltag Laboratories) containing ~1000 beads/μl. After staining of samples and acquisition of FACS data equivalent to 5000 counting beads, absolute cell numbers were calculated.

Statistical analysis

Data were analyzed using two-tailed Student's *t* test. All analyses were performed using Prism software (GraphPad Prism). Differences were considered significant at a p value <0.05. The slopes of IgG curves were compared by means of a mixed model ANOVA accounting for repeated measures.

Results

Generation of VLP-VSV

VLP-VSV were generated by transient cotransfection of 293FT cells with the MLV *gag/pol* expression plasmid pHIT60 together with the VSV-G expression construct pmDG. To obtain control particles, the EGF display construct pDEGF was used instead of pmDG (19). After 48-h incubation, cell culture supernatant was harvested and particles were concentrated by low speed centrifugation. Immunoelectron

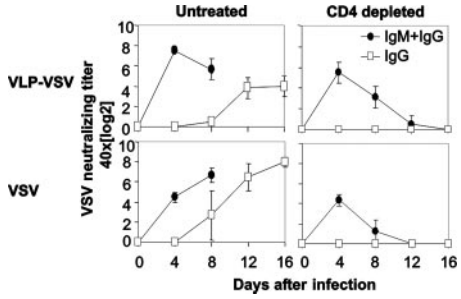

FIGURE 2. Similar to VSV, VLP-VSV induces a T help-independent neutralizing IgM response that switches T help dependently to IgG. For depletion of $CD4^+$ T cells, WT mice were treated i.p. with the mAb GK1.5 on days 3 and 1 before i.v. injection of VLP-VSV or VSV. Serum samples were collected at the indicated time points, and VSV-neutralizing IgM + G (●) or IgG (□) Abs were determined by a neutralization assay. Data shown are the mean of three mice per group ± SEM. One of two similar experiments is shown.

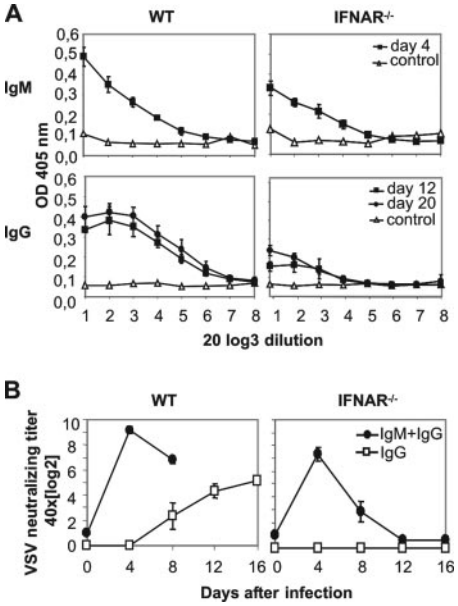

FIGURE 3. In the absence of a functional type I IFN system, VLP-VSV induces a VSV-specific IgM response, but no switch to IgG. WT and $IFNAR^{-/-}$ mice were immunized i.v. with VLP-VSV, and serum samples were taken on the indicated time points. *A*, VSV binding was analyzed by an ELISA method. Serum samples were taken on days 12 and 20 and tested in $\log_3$ serial dilutions (20-fold prediluted) for the presence of VSV-G-specific IgM or IgG. *B*, VSV-neutralizing Abs were determined by a neutralization assay. On indicated days, blood was taken and the serum was analyzed for the presence of VSV-neutralizing IgM + G (●) or IgG (□) Abs. Data shown are the mean of three mice per group ± SEM. One of two similar experiments is shown.

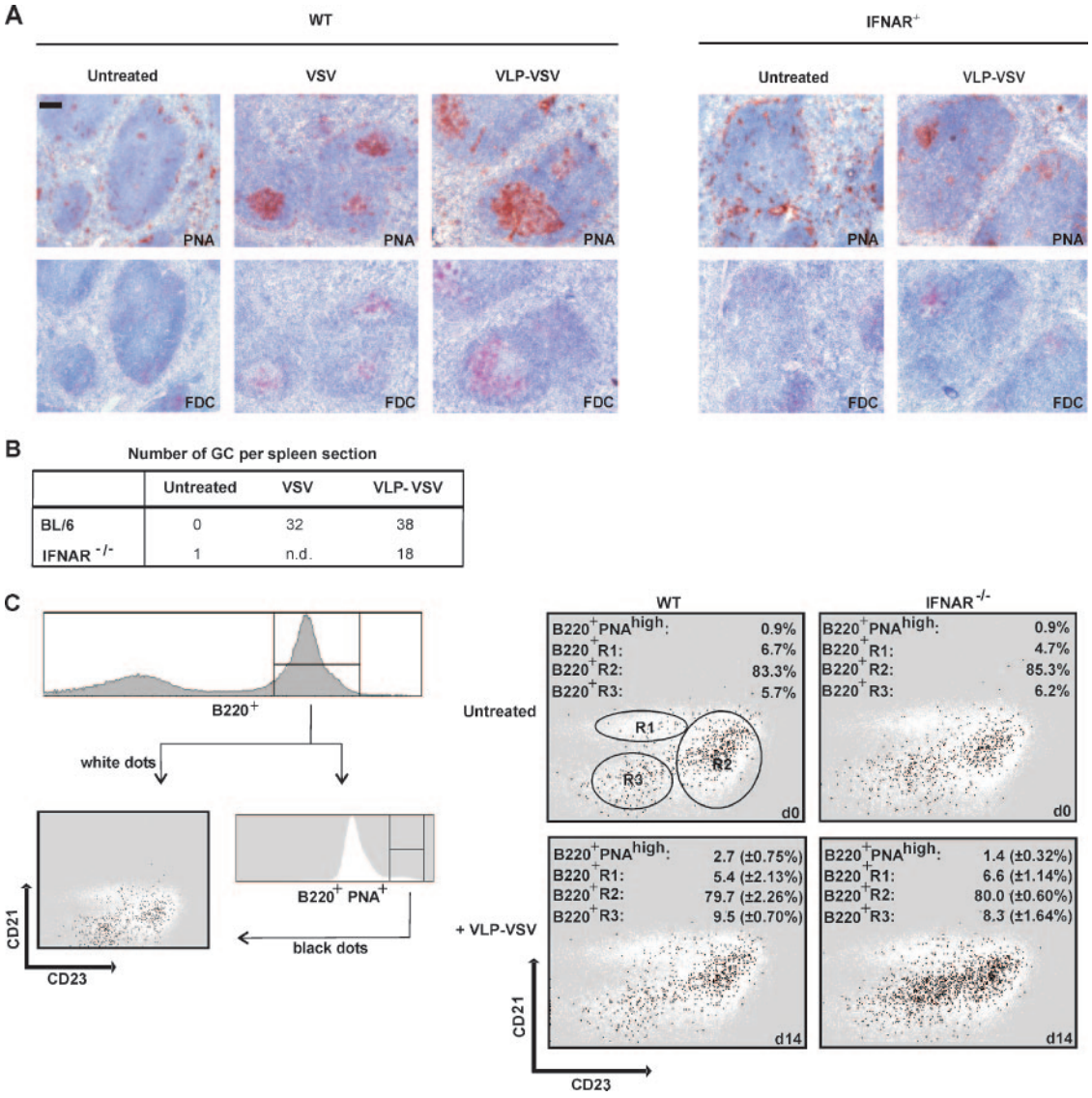

FIGURE 4. IFNAR$^{-/-}$ mice show a reduced GC formation after VLP-VSV immunization. *A*, Histological analysis of GC formation after i.v. immunization with VLP-VSV. Representative sections of spleens from mice treated with or without VLP-VSV 14 days after immunization were analyzed. The stained markers are indicated in each panel. Micrographs were taken at an original magnification of ×110; the bar is equivalent to 100 μm. *B*, Number of GC per spleen section. Spleens were analyzed for the presence of GC. Sections from two to three different mice were analyzed. *C*, Expression of B220$^+$PNA^{high} GC B cells after VLP-VSV immunization in WT and IFNAR$^{-/-}$ mice by FACS analysis. Cells were stained with anti-B220 PE Cy5.5, anti-CD21 FITC, anti-CD23 allophycocyanin Abs, and PNA streptavidin-PE. In FACS analysis, B220$^+$ B cells (white dots) were examined for the expression of CD21 and CD23 to identify CD21$^+$CD23^{low} marginal zone B cells (R1), CD21^{int}CD23^{high} follicular B cells (R2), and CD21^{low}CD23^{low} transitional B cells (R3). Furthermore, B220$^+$ B cells were analyzed for PNA binding. In the CD21/CD23 diagram, B220$^+$PNA^{high} cells are shown as black dots. Representative data are shown of splenocytes from naive mice (d0) or VLP-VSV-immunized mice (d14). The shown values represent mean percentages ± SEM of three mice of one representative experiment of three.

microscopic analysis revealed that VSV and VLP-VSV, but not VLP-EGF, were decorated by polyclonal rabbit serum specifically binding VSV-G (Fig. 1*A*). Upon coating of serially diluted VSV, VLP-VSV, and VLP-EGF on ELISA plates and incubation with the VSV-neutralizing mAb VI24, only VSV and VLP-VSV, but not VLP-EGF, showed binding of VI24. Staining with a VLP-specific anti-p30 serum was positive only for VLP-VSV and VLP-EGF, but not for VSV (Fig. 1*B*). Thus, VLP-VSV displayed VSV-G in a way that neutralizing determinants, as recognized by VI24 in an ELISA, were expressed.

Reminiscent of VSV, VLP-VSV induces a VSV-neutralizing IgM response that switches T help dependently to the IgG subclass

To analyze VSV-specific Ab responses induced by VLP-VSV, WT mice were i.v. injected with VLP-VSV or VSV, and serum samples were collected at the indicated time points. Determination of VSV-neutralizing serum titers revealed that within 4 days after injection of VLP-VSV, WT mice mounted VSV-neutralizing IgM that switched to the IgG subclass by day 12 and remained elevated (Fig. 2). Similarly, VSV-injected mice mounted neutralizing IgM by day 4 that switched to IgG by day 8 and remained elevated. VLP-VSV-induced IgM responses were slightly enhanced when compared with those induced by VSV, whereas IgG responses were ~2–4 $\log_2$ steps lower than those induced by VSV (Fig. 2). To analyze the T help dependence of VLP-VSV-induced Ab responses, untreated control mice and mice depleted of CD4$^+$ T cells were immunized with VSV or VLP-VSV, and neutralizing serum Abs were determined. As described previously (25), upon VSV infection of CD4-depleted mice, VSV-neutralizing IgM, but no

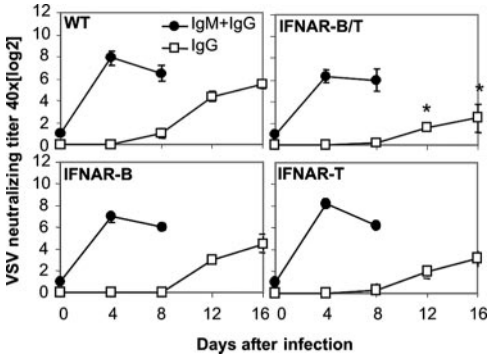

FIGURE 5. Direct IFNAR triggering lymphocytes has no impact on the VLP-VSV-induced IgG subclass switch. Mice with a cell type-specific type I IFN receptor ablation in B and T lymphocytes (CD19-Cre$^{+/-}$ CD4-Cre$^{+/-}$IFNAR$^{flox/flox}$; IFNAR-BT), or only in B cells (CD19-Cre$^{+/-}$IFNAR$^{flox/flox}$; IFNAR-B), or only in T cells (CD4-Cre$^{+/-}$ IFNAR$^{flox/flox}$; IFNAR-T) were immunized i.v. with VLP-VSV, and VSV-neutralizing IgM + G (●) or IgG (□) Abs were determined at the indicated time points in a neutralization assay. Data shown are the mean of three mice per group ± SEM. The slopes of the IgG curves of IFNAR-B and WT mice are statistically significantly higher than those of IFNAR-BT and IFNAR-T mice ($p = 0.0003$). Moreover, the absolute neutralization titers on days 12 and 16 of IFNAR-BT mice are significantly reduced when compared with the other groups (*, $p = 0.0046$).

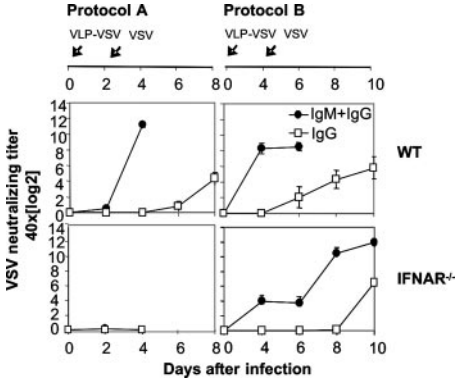

FIGURE 6. VLP-VSV-primed IFNAR$^{-/-}$ mice mount neutralizing IgG Abs after VSV challenge. WT and IFNAR$^{-/-}$ mice were first injected i.v. with VLP-VSV particles. Two (Protocol A) or 4 days (Protocol B) later, mice were challenged with 2×10^6 PFU of live VSV. Serum samples were collected at the indicated time points, and VSV-neutralizing IgM + G (●) or IgG (□) Abs were determined by a neutralization assay. Data shown are the mean of three mice per group ± SEM. One of two similar experiments is shown.

switch to IgG, was observed. Similarly, VLP-VSV-immunized mice devoid of CD4$^+$ T cells showed a neutralizing IgM response, but no IgG switch (Fig. 2). VSV- and VLP-VSV-induced IgM responses were slightly reduced in CD4-depleted mice when compared with untreated controls. Collectively, these results indicated that VSV and VLP-VSV induced T help-independent IgM responses that switched to IgG in a T help-dependent manner.

In VLP-VSV-immunized mice, the T help-dependent IgG switch is IFNAR dependent

To assess the IFNAR dependence of VLP-VSV-induced Ab responses, WT controls and IFNAR$^{-/-}$ mice were injected with VLP-VSV, and serum samples were collected at the indicated time points. VSV-specific Ig binding was assessed by applying serially diluted serum samples to plates coated with purified VSV. Specifically, bound IgM or IgG was detected by using goat anti-mouse IgM or goat anti-mouse IgG conjugated with HRP. Compared with WT controls, VLP-VSV-injected IFNAR$^{-/-}$ mice showed slightly reduced VSV-specific IgM titers on day 4, whereas VSV-specific IgG titers on days 12 and 20 were significantly reduced (Fig. 3*A*). Similarly, neutralizing IgM responses were only slightly reduced in IFNAR$^{-/-}$ mice when compared with WT mice. In contrast, the switch to neutralizing IgG and the sustained IgG production at later time points were entirely missing in VLP-VSV-treated IFNAR$^{-/-}$ mice (Fig. 3*B*). Thus, upon VLP-VSV immunization, the induction of neutralizing IgM was largely IFNAR independent, whereas the T help-dependent switch to neutralizing IgG was strictly IFNAR dependent.

IFNAR$^{-/-}$ mice showed a moderately reduced GC formation after VLP-VSV immunization

Because GC play a key role in subclass switch, GC formation was studied in WT controls and IFNAR$^{-/-}$ mice. To this end, mice were injected with VSV or VLP-VSV, and 14 days later spleens were prepared for immunohistological analysis. GC were identified by colocalization of PNA (Fig. 4*A*, *upper panels*) and FDC staining on consecutive sections (Fig. 4*A*, *lower panels*). Spleens of untreated WT and IFNAR$^{-/-}$ mice basically did not show GC, whereas after VLP-VSV or VSV immunization ~32 and 38 GC per section were found in WT spleens, respectively (Fig. 4, *A* and *B*). Upon VLP-VSV immunization, IFNAR$^{-/-}$ spleens showed ~18 GC per section (Fig. 4*B*).

The presence of GC B cells was further evaluated by flow cytometric analysis. Fourteen days after VLP-VSV or PBS treatment, splenocytes of IFNAR$^{-/-}$ mice and WT controls were stained with anti-B220, anti-CD21, anti-CD23, and PNA (Fig. 4*C*). FACS analysis revealed that PBS-treated WT mice showed ~0.9% B220$^+$PNA^{high} GC B cells, whereas 14 days after VLP-VSV treatment 2.7% B220$^+$PNA^{high} GC B cells were detected. B220$^+$ PNA^{high} GC B cells were primarily found among CD21^{int} CD23^{high} and CD21^{low}CD23^{low} B cells that are referred to as follicular B cells and transitional B cells, respectively. In contrast, B220$^+$PNA^{high} GC B cells were only rarely found among CD21^{high} CD23^{low} marginal zone B cells (Fig. 4*C*). In untreated IFNAR$^{-/-}$ mice, 0.9% B220$^+$PNA^{high} GC B cells were detected, whereas 14 days after VLP-VSV injection 1.4% B220$^+$PNA^{high} GC B cells were found. Also, in IFNAR$^{-/-}$ mice, the majority of B220$^+$PNA^{high} GC B cells were located among CD21^{int}CD23^{high} and CD21^{low}CD23^{low} B cells (Fig. 4*C*). Overall, the distribution of marginal zone B cells

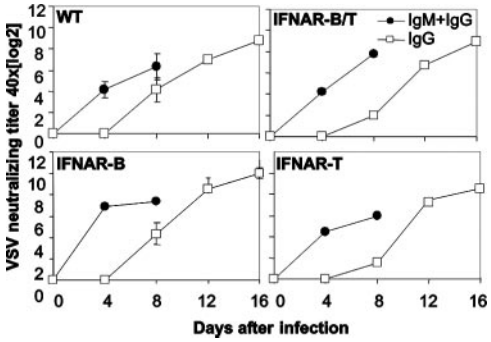

FIGURE 7. Mice with a lymphocyte-specific IFNAR ablation mount normal neutralizing Ab responses after VSV infection. WT, IFNAR-BT, IFNAR-B, and IFNAR-T mice were injected i.v. with 2×10^6 PFU of VSV, and VSV-neutralizing IgM + G (●) or IgG (□) serum titers were determined at the indicated time points in a neutralization assay. Data shown are the mean of three mice per group ± SEM.

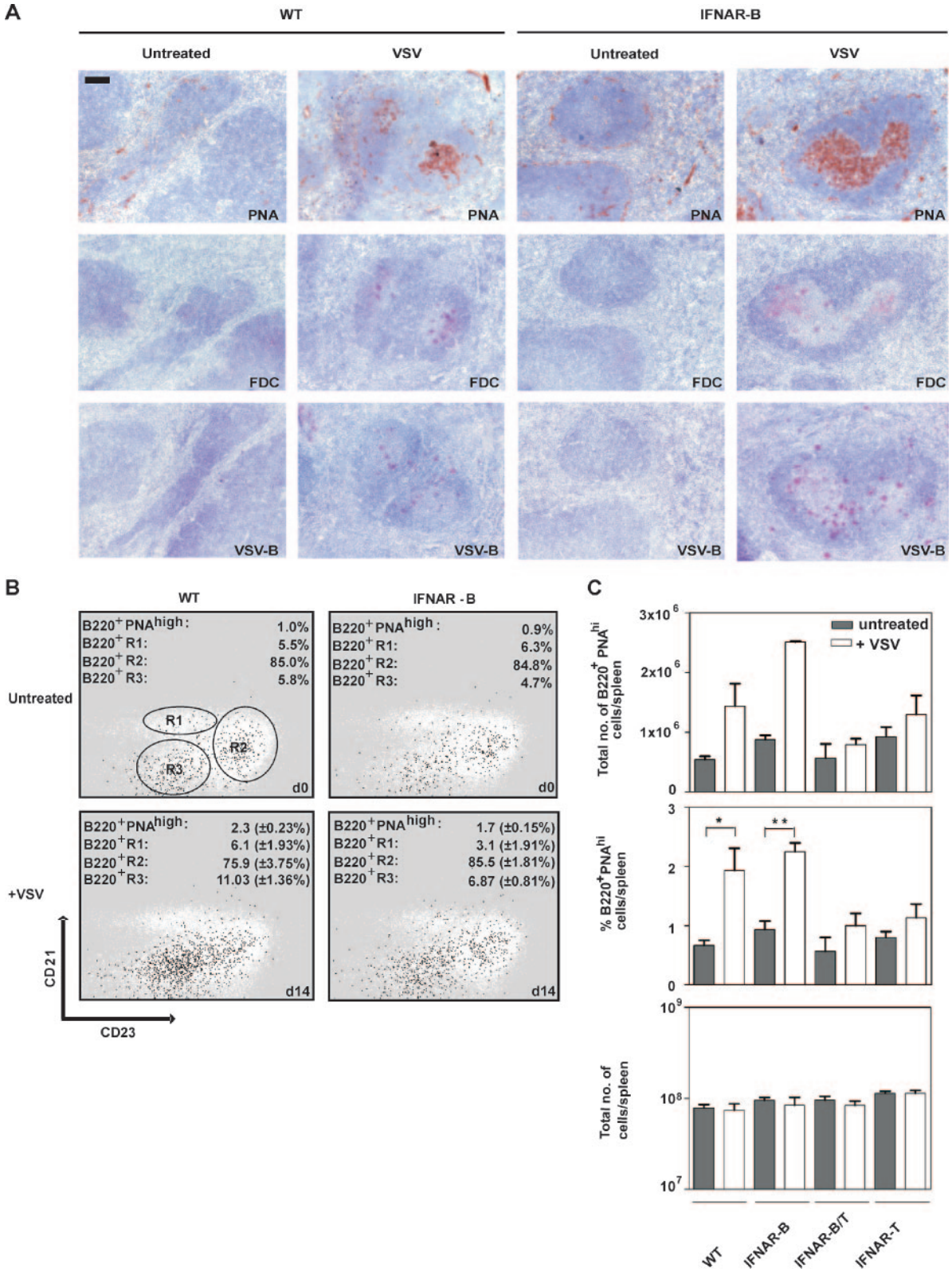

FIGURE 8. VSV-infected mice with a B lymphocyte-specific IFNAR ablation show a normal GC formation. *A*, Histological analysis of GC formation after VSV infection. Representative sections of spleens from mice treated with or without VSV were analyzed 14 days after VSV infection. Stained markers are indicated in each panel, including VSV-B, VSV-specific B cells. Micrographs were taken at an original magnification of ×110; the bar is equivalent to 100 μm. *B*, FACS analysis of PNA^{high} $B220^+$ GC B cells after VSV infection of WT and IFNAR-B mice. Data shown are representative stainings of spleen cells from naive mice (d0) or VSV-infected mice (d14). Cells were stained with anti-B220 PE Cy5.5, anti-CD21 FITC, anti-CD23 allophycocyanin Abs, and PNA streptavidin-PE. PNA^{high} GC B cells were analyzed among $B220^+$ B lymphocytes (black dots). Data represent mean percentages ± SEM of three mice of one representative experiment of three. *C*, Total spleen cell counts as well as absolute cell numbers and percentages of PNA^{high} GC B cells per spleen were analyzed for WT, IFNAR-B, IFNAR-BT, and IFNAR-T mice before and after VSV injection (*, $p < 0.0304$ WT vs WT + VSV; **, $p <$ 0,0091 IFNAR-B vs IFNAR-B + VSV). Data represent mean percentages ± SEM of three mice.

and follicular B cells of ~5–7% and 80–85%, respectively, did not change significantly in WT and IFNAR$^{-/-}$ mice upon VLP-VSV treatment, whereas CD21^{low}CD23^{low} B cells showed a slight increase in immunized mice. In conclusion, the immunohistological analysis and FACS studies showed that VLP-VSV treatment induced a GC reaction that was moderately reduced in IFNAR$^{-/-}$ mice when compared with WT controls.

The VLP-VSV-induced IFNAR-dependent IgG switch is largely independent of direct IFNAR triggering of lymphocytes

Because the VLP-VSV-induced IgG switch was T help dependent, we next addressed whether direct IFNAR triggering of T and/or B cells played a critical role. To this end, conditional knockout mice with a T cell (IFNAR-T), a B cell (IFNAR-B), or a combined B and T cell-specific (IFNAR-BT) IFNAR ablation were injected with VLP-VSV. Interestingly, all analyzed cell type-specific IFNAR-deficient mouse lines showed an IgG switch, although IgG responses in IFNAR-BT mice were statistically significantly reduced when compared with IFNAR-B, IFNAR-T, and WT controls (Fig. 5). Thus, direct IFNAR triggering of B cells or T cells was not critically required to promote the VLP-VSV-induced IgG switch. Nevertheless, reduced IgG levels observed in IFNAR-BT mice suggested that IFNAR triggering of both lymphocyte subsets further improved the IgG switch.

VLP-VSV-primed IFNAR$^{-/-}$ mice boosted with live VSV mount neutralizing IgG

To address whether in complete absence of a functional type I IFN system the subclass switch of neutralizing Ab responses could be induced at all, WT and IFNAR$^{-/-}$ mice were primed with VLP-VSV and challenged with VSV. After VLP-VSV priming and VSV challenge of WT mice, VSV-neutralizing IgM was induced by day 4 and significant IgG titers were detected after 8 days (Fig. 6, Protocols A and B). When IFNAR$^{-/-}$ mice were VSV challenged 2 days after VLP-VSV treatment, no neutralizing Abs were induced and mice succumbed to infection by day 4 (Protocol A). In contrast, mice that were VSV challenged 4 days after VLP-VSV priming survived for a total of 10 days before first signs of disease became apparent and the experiment had to be discontinued. Under such conditions, day 10 serum showed neutralizing IgG in all animals tested that reached a similar magnitude as compared with WT controls (Fig. 6, Protocol B). Thus, IFNAR$^{-/-}$ mice were able to mount neutralizing IgG responses, if stimulated appropriately.

VSV-infected mice with a lymphocyte-specific IFNAR deletion mount normal VSV-neutralizing IgM and IgG responses

To study whether upon VSV infection direct IFNAR triggering of B and/or T cells played a role, conditional knockout mice with a lymphocyte-specific IFNAR ablation were VSV infected and blood samples were collected at the indicated time points. Interestingly, IFNAR-BT as well as IFNAR-B or IFNAR-T mice mounted neutralizing Ab responses that were very similar to those of VSV-infected WT mice (Fig. 7). Immunohistological analysis of spleen sections prepared 14 days after VSV infection revealed a normal GC formation in IFNAR-B mice (Fig. 8*A*). In addition, numbers of GC per spleen section were similar in IFNAR-B mice and WT controls (~41 and 32 GC, respectively). Furthermore, FACS analysis showed a normal increase of 0.9% B220^{+}PNA^{high} GC B cells in untreated IFNAR-B mice to 1.7% B220^{+}PNA^{high} GC B cells in VSV-infected IFNAR-B mice (Fig. 8*B*). In a next step, IFNAR-B, IFNAR-BT, and IFNAR-T mice were analyzed for absolute counts and relative percentages of PNA^{high} GC B cells (Fig. 8*C*). As expected, WT and conditional knockout mice with a lymphocyte-specific IFNAR ablation showed an increase of B220^{+}PNA^{high} GC B cells 14 days after VSV injection that was more pronounced in WT and IFNAR-B mice compared with IFNAR-BT and IFNAR-T mice. Quantification of absolute cell counts showed similar amounts of splenocytes in WT and conditional knockout animals before and after immunization. Thus, after VSV infection, direct type I IFN stimulation of B cells is not critically required for the induction of neutralizing IgM responses.

Discussion

In this study, we demonstrate that VSV-neutralizing Ab responses induced by VLP-VSV showed a T help-dependent IgG switch that was critically dependent on IFNAR signaling. Although IFNAR triggering of lymphocytes is not a limiting step, it may gradually enhance the IgG switch. In VSV-infected mice, IFNAR triggering of B cells does neither critically affect GC formation nor the IgG switch of neutralizing Ab responses.

Several vaccination studies performed by Proietti et al. (8), Le Bon et al. (10, 11), and others indicated earlier that type I IFN stimulation may potently enhance Ab responses. In this study, we addressed whether virus-induced IFN-$\alpha\beta$ responses had an impact on the induction of neutralizing Ab responses. This question is of particular interest, because virus particles often display highly ordered Ags that induce T help-independent IgM responses, whereas the switch to the IgG subclass is T help dependent. Thus, compared with soluble Ags that induce IgM and IgG responses in a T help-dependent manner, it is a matter of question as to whether observations made with CGG similarly applied to Ab responses induced by virus particles. Usually a time gap of several days exists between the induction of IFN-$\alpha\beta$ responses and the appearance of neutralizing serum Abs. Therefore, it is important to understand whether early IFN-$\alpha\beta$ affects only early events such as the induction of IgM responses in primary foci or by local B cells. Alternatively, IFN-$\alpha\beta$ could also have an impact on later immune reactions, such as the IgG switch of protective neutralizing Ab responses. Because IFNAR$^{-/-}$ mice, which have been instrumental in studying IFN-$\alpha\beta$ effects in vivo, are extremely sensitive to lethal VSV infection (4), we generated VLP-VSV that are entirely replication deficient and thus are noninfective. Compared with UV-inactivated VSV that induces IgM, but no IgG responses at a broad range of doses, we showed in this study and in a previous report (21) that VLP were highly immunogenic and induced Ab responses comprising IgM and IgG subclasses.

VLP-VSV-induced Ab responses that showed a T help-dependent switch of neutralizing IgM to IgG were critically dependent on IFNAR triggering. Interestingly, under these conditions, IFNAR signaling on the level of B or T cells did not critically contribute to the IgG switch. The observation that mice with a combined B and T cell-specific IFNAR ablation showed moderately reduced neutralizing Ab responses upon VLP-VSV immunization suggested that IFNAR signaling on lymphocytes may synergize to further improve the IgG switch.

Conditional IFNAR mice with a B cell-, T cell-, or combined B and T cell-specific IFNAR ablation infected with VSV mounted normal neutralizing IgM and IgG responses. This observation is in contrast to a recent study by Fink et al. (15), who observed reduced VSV-specific IgM responses in the absence of IFNAR signaling. In this study, mice were used that carried 3×10^6 adoptively transferred VSV-specific B cells that were IFNAR proficient or deficient. It was shown that upon in vitro incubation of IFNAR-deficient splenocytes with VSV, any cell type, including specific and nonspecific B cells, macrophages, plasmacytoid DCs, and DCs, was readily infected. In contrast, IFNAR-competent splenocytes showed a strikingly reduced infection with basically only VSV-specific B cells and to a lesser extent unspecific B cells being

infected. Thus, it is likely that in this system the 3×10^6 adoptively transferred IFNAR-deficient B cells bound a good proportion of the 2×10^6 PFU injected VSV that then resulted in infection of the B cells and subsequent cell lysis. In conclusion, it is possible that in mice carrying adoptively transferred IFNAR-deficient B cells, VSV-induced Ab responses were reduced due to experimental conditions that favored VSV infection of VSV-specific and IFNAR-deficient B cells.

In the mouse model we studied, IFNAR-B mice showed a polyclonal B cell repertoire. Thus, in IFNAR-B mice, effects as discussed above are unlikely to take place. Assuming the presence of $>10^9$ B cells in a mouse, basically all of which are IFNAR deficient (3, 10), $<0.1\%$ of the B cells can theoretically get infected upon injection of 2×10^6 PFU VSV. Because, in absence of IFNAR, VSV-specific B cells do not seem to get preferentially infected (15), this would result in the infection and destruction of $<0.1\%$ of the VSV-specific B cell repertoire. Thus, the observations described in this work probably reflect the in vivo conditions more appropriately than adoptive transfer experiments.

Upon BCR cross-linking in vitro, type I IFN was shown to increase the sensitivity of naive B cells to produce IgM (7). This suggested a lowered threshold for the induction of T help-independent IgM responses. Upon VLP-VSV immunization, IFNAR$^{-/-}$ mice raised slightly reduced IgM responses when compared with WT mice. Nevertheless, IFNAR-B mice did not show such a difference. Thus, in the case of the highly repetitive T cell-independent VSV-G surface Ag, optimal conditions for BCR cross-linking are provided (6, 26) that cannot be further enhanced by IFN-$\alpha\beta$ stimulation. This is in contrast to the T cell-dependent Ag CGG, as discussed previously (10).

A study by Coro et al. (14) showed that influenza virus infection induced early local Ab responses that were dependent on B cell-specific IFNAR signaling. In this study, a low pathogenic influenza virus strain was used that was similarly well cleared in IFNAR$^{-/-}$ and WT mice and thus allowed a comparative analysis of influenza virus-specific B cell responses in both mouse strains. In this model, IgG isotype profiles were changed in IFNAR$^{-/-}$ mice. Because to date isotype profiles have been found to be affected by IFN-γ, but not by IFN-$\alpha\beta$, it was possible that in this model type I and type II IFN cross-talk played a role (27). In another model, LCMV infection induced similar Ig responses against NP in IFNAR$^{-/-}$ and WT mice (13). Although type I IFN responses are induced by LCMV (12), these results suggested that in the case of LCMV-induced Ab responses, IFNAR triggering did not play a role.

We report a previously unrecognized role of IFNAR triggering for the subclass switch of VSV-neutralizing Ab responses, using a nonproductive viral infection. Unlike vaccination with CGG in type I IFN (10), in our model exogenous administration of type I IFN was not required for the induction of early T help-independent IgM responses. Hence, for IgM production, the immunogenicity of VLP-VSV was functionally redundant with the adjuvant activity of type I IFN.

The IFNAR dependence of VLP-VSV-induced IgG switch raised the question as to how VLPs induce type I IFN responses. Because VLPs have been reported to contain cellular RNA instead of genomic RNA (28), it will be of interest how such particles trigger host innate immunity. The mild lymphopenia and concomitant CD69 up-regulation observed in blood of VLP-VSV-vaccinated animals suggested stimulation with locally effective, but systemically limited quantities of type I IFN (data not shown). Notwithstanding, the mild reduction in IFNAR$^{-/-}$ lymphocyte numbers hints at the induction of other cytokines as well. We think that our observations with VLP-VSV are relevant for VSV infection because VLP-VSV and VSV similarly express VSV-neutralizing determinants. This is supported by the observation that upon pseudotyping of retroviral and lentiviral vectors, VSV-G forms a fully functional trimeric complex that mediates cell entry and membrane fusion (29). One difference of VLP-VSV compared with VSV is the amount of VSV-G expressed per virus-like particle, which is likely to be higher in VSV: bullet-shaped VSV displays strictly ordered gp in a paracrystalline manner, whereas on spherically shaped VLPs, VSV-G is probably less ordered. Nevertheless, these differences are not expected to significantly affect the expression of VSV-neutralizing epitopes, as also supported by electronmicroscopic studies in which a polyclonal anti-VSV-G serum decorated VSV and VLP-VSV, but not VLP-EGF (Fig. 1*A*). Furthermore, Ab responses induced by VLP-VSV or VSV were analyzed for virus-neutralizing activity using one and the same live VSV-IND isolate in all tests. Thus, although VLP-VSV and VSV are considerably divergent reagents, the overall quality of Ab responses induced by these reagents can be directly compared.

Possible mechanisms by which type I IFN promotes subclass switch could involve recruitment of lymphocytes into B and T cell zones (3) and improvement of B cell priming and the GC formation through up-regulation of the costimulatory molecules CD40-CD40L, OX40-OX40L, CD80, or CD86-CD28 on DCs and B and T lymphocytes (30–32). Alternatively, immunological synapse formation could further be improved by stronger interactions between LFA-1 and ICAM-1 (3). Type I IFN stimulation enhances B cell survival in vitro (33) and could hence rescue B cells from apoptosis in vivo, an effect that was identified recently in CD8$^+$ T cells as a crucial mechanism to promote the generation of CTL (34). Finally, virus infection may activate plasmacytoid DCs to secrete IFN-$\alpha\beta$, which supports generation of non-Ig-secreting plasma blasts and IL-6 to promote differentiation into Ig-secreting plasma cells (35).

In conclusion, Ab responses that differ with respect to their IFNAR dependence are induced, depending on the nature of the administered Ag. Low immunogenic Ags such as CGG induce significantly improved Ab responses if coadministered with type I IFN. Under such conditions, type I IFN has a direct impact on APCs, T cells, and B cells. In contrast, VLP-VSV that is more immunogenic, but replication deficient, induced an IFNAR-dependent IgG switch. Under such conditions, lymphocyte-specific IFNAR triggering played a very minor role. Local infection with low pathogenic influenza virus required IFNAR triggering of B cells. In this model, it is possible that IFN-γ and IFN-$\alpha\beta$ cross-talk played a role. Finally, replication-competent LCMV or VSV induced Ab responses that were largely independent of B cell-specific IFNAR triggering. Hence, an overall strong immune activation could compensate for the lack of type I IFN stimulation. Indeed, considering that many viruses have developed means to interfere with the induction of type I IFN (36–41), it seems likely that some kind of functional redundancy has evolved to guarantee the efficient induction of protective anti-viral Ab responses.

Acknowledgments

We thank Dorothea Kreuz for expert technical assistance and Norbert Wey for help with the preparation of micrographs.

Disclosures

The authors have no financial conflict of interest.

References

1. Kawai, T., and S. Akira. 2006. Role of IPS-1 in type I IFN induction. *Nippon Rinsho* 64: 1231–1235.
2. Barchet, W., M. Cella, B. Odermatt, C. Asselin-Paturel, M. Colonna, and U. Kalinke. 2002. Virus-induced interferon α production by a dendritic cell subset in the absence of feedback signaling in vivo. *J. Exp. Med.* 195: 507–516.

3. Kamphuis, E., T. Junt, Z. Waibler, R. Forster, and U. Kalinke. 2006. Type I interferons directly regulate lymphocyte recirculation and cause transient blood lymphopenia. *Blood* 108: 3253–3261.
4. Muller, U., U. Steinhoff, L. F. Reis, S. Hemmi, J. Pavlovic, R. M. Zinkernagel, and M. Aguet. 1994. Functional role of type I and type II interferons in antiviral defense. *Science* 264: 1918–1921.
5. Thomsen, A. R., A. Nansen, C. Andersen, J. Johansen, O. Marker, and J. P. Christensen. 1997. Cooperation of B cells and T cells is required for survival of mice infected with vesicular stomatitis virus. *Int. Immunol.* 9: 1757–1766.
6. Bachmann, M. F., and R. M. Zinkernagel. 1997. Neutralizing antiviral B cell responses. *Annu. Rev. Immunol.* 15: 235–270.
7. Braun, D., I. Caramalho, and J. Demengeot. 2002. IFN-$\alpha\beta$ enhances BCR-dependent B cell responses. *Int. Immunol.* 14: 411–419.
8. Proietti, E., L. Bracci, S. Puzelli, T. Di Pucchio, P. Sestili, E. De Vincenzi, M. Venditti, I. Capone, I. Seif, E. De Maeyer, et al. 2002. Type I IFN as a natural adjuvant for a protective immune response: lessons from the influenza vaccine model. *J. Immunol.* 169: 375–383.
9. Le Bon, A., G. Schiavoni, G. D'Agostino, I. Gresser, F. Belardelli, and D. F. Tough. 2001. Type I interferons potently enhance humoral immunity and can promote isotype switching by stimulating dendritic cells in vivo. *Immunity* 14: 461–470.
10. Le Bon, A., C. Thompson, E. Kamphuis, V. Durand, C. Rossmann, U. Kalinke, and D. F. Tough. 2006. Cutting edge: enhancement of antibody responses through direct stimulation of B and T cells by type I IFN. *J. Immunol.* 176: 2074–2078.
11. Le Bon, A., V. Durand, E. Kamphuis, C. Thompson, S. Bulfone-Paus, C. Rossmann, U. Kalinke, and D. F. Tough. 2006. Direct stimulation of T cells by type I IFN enhances the $CD8^+$ T cell response during cross-priming. *J. Immunol.* 176: 4682–4689.
12. Malmgaard, L., T. P. Salazar-Mather, C. A. Lewis, and C. A. Biron. 2002. Promotion of $\alpha\beta$ interferon induction during in vivo viral infection through $\alpha\beta$ interferon receptor/STAT1 system-dependent and -independent pathways. *J. Virol.* 76: 4520–4525.
13. Van den Broek, M. F., U. Muller, S. Huang, R. M. Zinkernagel, and M. Aguet. 1995. Immune defense in mice lacking type I and/or type II interferon receptors. *Immunol. Rev.* 148: 5–18.
14. Coro, E. S., W. L. Chang, and N. Baumgarth. 2006. Type I IFN receptor signals directly stimulate local B cells early following influenza virus infection. *J. Immunol.* 176: 4343–4351.
15. Fink, K., K. S. Lang, N. Manjarrez-Orduno, T. Junt, B. M. Senn, M. Holdener, S. Akira, R. M. Zinkernagel, and H. Hengartner. 2006. Early type I interferon-mediated signals on B cells specifically enhance antiviral humoral responses. *Eur. J. Immunol.* 36: 2094–2105.
16. Lee, P. P., D. R. Fitzpatrick, C. Beard, H. K. Jessup, S. Lehar, K. W. Makar, M. Perez-Melgosa, M. T. Sweetser, M. S. Schlissel, S. Nguyen, et al. 2001. A critical role for Dnmt1 and DNA methylation in T cell development, function, and survival. *Immunity* 15: 763–774.
17. Rickert, R. C., J. Roes, and K. Rajewsky. 1997. B lymphocyte-specific, Cre-mediated mutagenesis in mice. *Nucleic Acids Res.* 25: 1317–1318.
18. Soneoka, Y., P. M. Cannon, E. E. Ramsdale, J. C. Griffiths, G. Romano, S. M. Kingsman, and A. J. Kingsman. 1995. A transient three-plasmid expression system for the production of high titer retroviral vectors. *Nucleic Acids Res.* 23: 628–633.
19. Naldini, L., U. Blomer, P. Gallay, D. Ory, R. Mulligan, F. H. Gage, I. M. Verma, and D. Trono. 1996. In vivo gene delivery and stable transduction of nondividing cells by a lentiviral vector. *Science* 272: 263–267.
20. Pyra, H., J. Boni, and J. Schupbach. 1994. Ultrasensitive retrovirus detection by a reverse transcriptase assay based on product enhancement. *Proc. Natl. Acad. Sci. USA* 91: 1544–1548.
21. Nikles, D., P. Bach, K. Boller, C. A. Merten, F. Montrasio, F. L. Heppner, A. Aguzzi, K. Cichutek, U. Kalinke, and C. J. Buchholz. 2005. Circumventing tolerance to the prion protein (PrP): vaccination with PrP-displaying retrovirus particles induces humoral immune responses against the native form of cellular PrP. *J. Virol.* 79: 4033–4042.
22. Kalinke, U., A. Oxenius, C. Lopez-Macias, R. M. Zinkernagel, and H. Hengartner. 2000. Virus neutralization by germ-line vs. hypermutated antibodies. *Proc. Natl. Acad. Sci. USA* 97: 10126–10131.
23. Charan, S., and R. M. Zinkernagel. 1986. Antibody mediated suppression of secondary IgM response in nude mice against vesicular stomatitis virus. *J. Immunol.* 136: 3057–3061.
24. Bachmann, M. F., B. Odermatt, H. Hengartner, and R. M. Zinkernagel. 1996. Induction of long-lived germinal centers associated with persisting antigen after viral infection. *J. Exp. Med.* 183: 2259–2269.
25. Leist, T. P., S. P. Cobbold, H. Waldmann, M. Aguet, and R. M. Zinkernagel. 1987. Functional analysis of T lymphocyte subsets in antiviral host defense. *J. Immunol.* 138: 2278–2281.
26. Bachmann, M. F., H. Hengartner, and R. M. Zinkernagel. 1995. T helper cell-independent neutralizing B cell response against vesicular stomatitis virus: role of antigen patterns in B cell induction? *Eur. J. Immunol.* 25: 3445–3451.
27. Takaoka, A., Y. Mitani, H. Suemori, M. Sato, T. Yokochi, S. Noguchi, N. Tanaka, and T. Taniguchi. 2000. Cross talk between interferon-γ and -$\alpha\beta$ signaling components in caveolar membrane domains. *Science* 288: 2357–2360.
28. Muriaux, D., J. Mirro, D. Harvin, and A. Rein. 2001. RNA is a structural element in retrovirus particles. *Proc. Natl. Acad. Sci. USA* 98: 5246–5251.
29. Cronin, J., X. Y. Zhang, and J. Reiser. 2005. Altering the tropism of lentiviral vectors through pseudotyping. *Curr. Gene Ther.* 5: 387–398.
30. Klaus, S. J., I. Berberich, G. Shu, and E. A. Clark. 1994. CD40 and its ligand in the regulation of humoral immunity. *Semin. Immunol.* 6: 279–286.
31. McAdam, A. J., E. A. Farkash, B. E. Gewurz, and A. H. Sharpe. 2000. B7 costimulation is critical for antibody class switching and $CD8^+$ cytotoxic T-lymphocyte generation in the host response to vesicular stomatitis virus. *J. Virol.* 74: 203–208.
32. Walker, L. S., A. Gulbranson-Judge, S. Flynn, T. Brocker, and P. J. Lane. 2000. Co-stimulation and selection for T-cell help for germinal centres: the role of CD28 and OX40. *Immunol. Today* 21: 333–337.
33. Morikawa, K., H. Kubagawa, T. Suzuki, and M. D. Cooper. 1987. Recombinant interferon-α, -β, and -γ enhance the proliferative response of human B cells. *J. Immunol.* 139: 761–766.
34. Kolumam, G. A., S. Thomas, L. J. Thompson, J. Sprent, and K. Murali-Krishna. 2005. Type I interferons act directly on CD8 T cells to allow clonal expansion and memory formation in response to viral infection. *J. Exp. Med.* 202: 637–650.
35. Jego, G., A. K. Palucka, J. P. Blanck, C. Chalouni, V. Pascual, and J. Banchereau. 2003. Plasmacytoid dendritic cells induce plasma cell differentiation through type I interferon and interleukin 6. *Immunity* 19: 225–234.
36. Abate, D. A., S. Watanabe, and E. S. Mocarski. 2004. Major human cytomegalovirus structural protein pp65 (ppUL83) prevents interferon response factor 3 activation in the interferon response. *J. Virol.* 78: 10995–11006.
37. Dauber, B., G. Heins, and T. Wolff. 2004. The influenza B virus nonstructural NS1 protein is essential for efficient viral growth and antagonizes β interferon induction. *J. Virol.* 78: 1865–1872.
38. DiPerna, G., J. Stack, A. G. Bowie, A. Boyd, G. Kotwal, Z. Zhang, S. Arvikar, E. Latz, K. A. Fitzgerald, and W. L. Marshall. 2004. Poxvirus protein N1L targets the I-κB kinase complex, inhibits signaling to NF-κB by the tumor necrosis factor superfamily of receptors, and inhibits NF-κB and IRF3 signaling by Toll-like receptors. *J. Biol. Chem.* 279: 36570–36578.
39. Foy, E., K. Li, C. Wang, R. Sumpter, Jr., M. Ikeda, S. M. Lemon, and M. Gale, Jr. 2003. Regulation of interferon regulatory factor-3 by the hepatitis C virus serine protease. *Science* 300: 1145–1148.
40. Ploegh, H. L. 1998. Viral strategies of immune evasion. *Science* 280: 248–253.
41. Stojdl, D. F., B. D. Lichty, B. R. tenOever, J. M. Paterson, A. T. Power, S. Knowles, R. Marius, J. Reynard, L. Poliquin, H. Atkins, et al. 2003. VSV strains with defects in their ability to shutdown innate immunity are potent systemic anti-cancer agents. *Cancer Cells* 4: 263–275.